


RESEARCH

Open Access



# Association of variants in the *KIF1A* gene with amyotrophic lateral sclerosis

Panlin Liao<sup>1†</sup>, Yanchun Yuan<sup>2†</sup>, Zhen Liu<sup>2</sup>, Xiaorong Hou<sup>2</sup>, Wanzhen Li<sup>2</sup>, Jin Wen<sup>1</sup>, Kexuan Zhang<sup>1</sup>, Bin Jiao<sup>2,3,4,5</sup>, Lu Shen<sup>2,3,4,5,6,7</sup>, Hong Jiang<sup>2,3,4,5</sup>, Jifeng Guo<sup>2,3,4,5</sup>, Beisha Tang<sup>2,3,4,5</sup>, Zhuohua Zhang<sup>1,3,5</sup>, Zhonghua Hu<sup>1,3,5,8,9\*</sup> and Junling Wang<sup>2,3,4,5,6,7\*</sup> 

## Abstract

**Background:** Amyotrophic lateral sclerosis (ALS) is a devastating progressive neurodegenerative disease that affects neurons in the central nervous system and the spinal cord. As in many other neurodegenerative disorders, the genetic risk factors and pathogenesis of ALS involve dysregulation of cytoskeleton and neuronal transport. Notably, sensory and motor neuron diseases such as hereditary sensory and autonomic neuropathy type 2 (HSAN2) and spastic paraplegia 30 (SPG30) share several causative genes with ALS, as well as having common clinical phenotypes. *KIF1A* encodes a kinesin 3 motor that transports presynaptic vesicle precursors (SVPs) and dense core vesicles and has been reported as a causative gene for HSAN2 and SPG30.

**Methods:** Here, we analyzed whole-exome sequencing data from 941 patients with ALS to investigate the genetic association of *KIF1A* with ALS.

**Results:** We identified rare damage variants (RDVs) in the *KIF1A* gene associated with ALS and delineated the clinical characteristics of ALS patients with *KIF1A* RDVs. Clinically, these patients tended to exhibit sensory disturbance. Interestingly, the majority of these variants are located at the C-terminal cargo-binding region of the *KIF1A* protein. Functional examination revealed that the ALS-associated *KIF1A* variants located in the C-terminal region preferentially enhanced the binding of SVPs containing RAB3A, VAMP2, and synaptophysin. Expression of several disease-related *KIF1A* mutants in cultured mouse cortical neurons led to enhanced colocalization of RAB3A or VAMP2 with the *KIF1A* motor.

**Conclusions:** Our study highlighted the importance of *KIF1A* motor-mediated transport in the pathogenesis of ALS, indicating *KIF1A* as an important player in the oligogenic scenario of ALS.

**Keywords:** Amyotrophic lateral sclerosis, *KIF1A*, Axonal transport, Presynaptic vesicle precursors

## Background

Amyotrophic lateral sclerosis (ALS) is a devastating neurodegenerative disease characterized by progressive degeneration of the upper and lower motor neurons, leading to muscular weakness and atrophy [1, 2]. ALS typically occurs in individuals between ages 42 and 65 and invariably leads to death due to respiratory failure three to four years after disease onset [1, 2]. Growing evidence shows that genetic risk factors, environmental exposure, and aging are implicated in the pathogenesis

<sup>†</sup>Panlin Liao and Yanchun Yuan contributed equally to this work

\*Correspondence: huzhonghua@csu.edu.cn; junling.wang@csu.edu.cn

<sup>1</sup> Hunan Key Laboratory of Molecular Precision Medicine, Department of Critical Care Medicine, Xiangya Hospital, Central South University, Changsha 410008, China

<sup>2</sup> Department of Neurology, Xiangya Hospital, Central South University, Changsha 410008, China

Full list of author information is available at the end of the article



of ALS [3, 4]. Approximately 10% of ALS cases are familial ALS (FALS), and the remaining cases are classified as sporadic ALS (SALS). In recent years, with the advent of next-generation sequencing technology, more than 40 genes have been discovered to be involved in the pathogenesis of ALS [3, 5].

Despite the increase in genetic insights and the characterization of numerous ALS-associated genes, the biological mechanisms underlying how ALS genes contribute to the ALS phenotype remain to be elucidated. Various lines of genetic, pathological and neurobiological evidence have identified axon transport deficits as essential pathogenic mechanisms for ALS [6]. First, many ALS-associated genes (such as *PFN1*, *TUBA4A*, *DCTN1*, *ALS2*, *NEFH*, *KIF5A*, and *SPAST*) are known to regulate cytoskeletal dynamics and function as well as intracellular transport events [3, 6–9]. Second, animal studies have shown that defects in axonal transport and distal axonal damage are key pathogenic features in ALS animal models and precede the ALS-like symptoms in these animals [10–15]. Third, neuropathological analysis has indicated that some ALS patients exhibit denervation and reinnervation changes in muscles but normal-appearing motor neurons, suggesting that axonal damage occurs earlier than the initial apparent symptoms in ALS, that is, before clinical manifestations of disease [16]. Moreover, axonal cytoskeletal disorganization and defective transportation have been reported in a series of other neurodegenerative diseases, such as spastic paraplegia (SPG), Charcot-Marie-Tooth disease, and Parkinson's disease [17, 18], highlighting axonal transport as a potential convergent mechanism of pathological neurodegeneration.

*KIF1A* encodes a kinesin-3 molecular motor [19] that transports both synaptic vesicle precursors (SVPs) carrying synaptic vesicle proteins (such as synaptophysin, VAMP2, and RAB3A) [20–22] and dense core vesicles (DCVs) carrying neuropeptides and neurotrophic factors [23–25]. *KIF1A* deficiency in mice leads to remarkable neuronal degeneration and death [26], indicating a pathogenic association with neurodegenerative conditions. Moreover, *KIF1A* heterozygous mutations have been linked to a variety of neurodegenerative and neurodevelopmental diseases [27]. Currently, mutations in *KIF1A* are listed as associated with three disorders in the OMIM database: hereditary sensory and autonomic neuropathy type 2 (HSAN2) with a recessive pattern; mental retardation type 9 (MRD9) with dominant inheritance; and SPG30 with either dominant or recessive inheritance. HSAN and SPG are known to share pathogenic genes with ALS. For example, *KIF5A* and *SPG11* are characterized as common causative genes of both ALS and SPG [28–31], and the *SPTLC1* gene, which causes HSAN, has recently been identified as a causative gene of

juvenile ALS [32, 33]. In addition, SPG overlaps with ALS in terms of clinical symptoms and genetic risk factors. Thus, we hypothesize that the *KIF1A*-related mutations are a genetic risk of ALS pathogenesis.

In this study, we performed whole-exome sequencing (WES) in 941 patients with ALS, validated the candidate variants in an additional publicly available cohort of 4366 patients with ALS. We identified rare damage variants (RDVs) in the *KIF1A* gene associated with ALS, and investigated the functional effects of these variants on axonal transport.

## Methods

### Patients and clinical analysis

In this study, 941 patients with ALS, including 55 FALS and 886 SALS patients, were enrolled for mutation screening of candidate genes. This ALS cohort included 753 ALS patients whom we had reported on previously [2]. Among these patients, pathogenic nucleotide repeat expansion mutations in *C9ORF72* and *ATXN2* were excluded by PCR and repeat-primer PCR analysis. A comprehensive battery of clinical data including age, sex, family history and clinical features such as age at onset (AAO), site of onset, disease duration, and ALS Functional Rating Scale–Revised score were collected from all participants. To perform burden analysis, we selected WES data from 6708 East Asian individuals without any neurological disease in the gnomAD database v2 as the control for our ALS Chinese cohort. In addition, burden analysis was also performed in the Project MinE cohort (including 4366 ALS patients and 1832 controls) [34, 35]. In addition, *KIF1A* variants were screened in an independent ALS cohort from a publicly available dataset (ALSdb, New York City, New York (URL: <http://alsdb.org>) [Mar, 2022]), which consists of 3317 SALS patients who have undergone WES [36].

### WES analysis

All patients with ALS underwent WES using a previously described method [2, 37]. Variants that failed to meet our quality control requirements (coverage depth < 10, allele balance < 0.25, and Phred quality score < 20) were excluded. RDV was included for further analysis if it was (1) located in the *KIF1A* gene; (2) rare, i.e., for heterozygous variants, a minor allele frequency (MRD) less than 0.1% in the 1000 Genomes Project, Exome Aggregation Consortium (ExAC) and gnomAD; for homozygous or compound heterozygous variants, a minor allele frequency (MAF) less than 1% in the above public databases; (3) a nonsynonymous, indel, or putative splice site variant; and (4) pathogenic. For SALS, the pathogenicity was predicted by ReVe, a pathogenicity-computation method [38], with an ReVe value more than 0.7; for FALS,

the pathogenicity was identified based on co-segregation results and prediction of ReVe. Then, the variants identified by WES were validated by Sanger sequencing.

#### Plasmids and reagents

To construct the pGW1-KIF1A-3xFLAG plasmid, *KIF1A* cDNA was obtained by RT-PCR from mRNA extracted from human embryonic stem cells and cloned into the pGW1 vector [39] between the EcoRI and HindIII sites. The FLAG tag sequence was added to the reverse primer during PCR. To generate the pGW1-KIF1A-Venus or the pGW1-RFP-RAB3A construct, the cDNAs of KIF1A and RAB3A were obtained by RT-PCR and cloned into the pGW1 vector between the EcoRI and HindIII sites by using the Gibson assembly method. The pCMV-3xFLAG-RAB3A plasmid was constructed by PCR amplifying RAB3A from pGW1-RFP-RAB3A and subcloning the PCR fragment into the 3xFLAG-pCMV vector (Sigma, St. Louis, MO; E7658) between the EcoRI and BamHI sites. KIF1A point variants were designed using the NEBase Changer website. All clones were sequenced, and the expression of correctly sized proteins was confirmed by Western blot. FLAG-VAMP2 and RFP-synaptophysin plasmids were as described previously [40, 41]. The primer sequences used for constructing these plasmids are listed in Additional file 1: Table S1.

The following antibodies were used: DYKDDDDK Tag (CST, Danvers, MA; 8146), GFP (Invitrogen, Waltham, MA; A11122), actin (CST, 4970S), tubulin (TransGen, Beijing, China, P10513), GAPDH (Abcam, Cambridge, United Kingdom, ab8245), RFP (Rockland, Limerick, PA; 600-401-379), Alexa Fluor 555 donkey anti-mouse IgG (H + L) (Invitrogen, A21422), goat anti-rabbit IgG-HRP (Absin, Shanghai, China, abs20040ss), and goat anti-mouse IgG-HRP (Absin, abs20039ss).

#### Coimmunoprecipitation

HEK293T cells were cultured in DMEM (Gibco, Waltham, MA; 11995500) supplemented with 10% fetal bovine serum (ProCell, Wuhan, China, 164210-50) and 100 U/ml penicillin–streptomycin solution (Thermo Fisher, Waltham, MA; 15140148). The cells were transfected using a GenJet instrument (SignaGen, Frederick, MD; SL100488) according to the manufacturer's instructions. Forty-eight hours after transfection, cells were lysed in coimmunoprecipitation buffer (20 mM Tris-HCl pH 7.5, 150 mM NaCl, 1 mM EGTA, 1% Triton X-100 and proteinase inhibitors) at 4 °C for 30 min and then centrifuged at 13,000 rpm at 4 °C for 30 min to separate the soluble and insoluble fractions. Approximately 10%–20% of the supernatant was used as the input control, and the remainder was used for immunoprecipitation. The input was mixed with 2 × Laemmli sample buffer

(60 mM Tris-HCl pH 6.8, 2% SDS, 10% glycerol, 5% β-mercaptoethanol, 0.01% bromophenol blue) and boiled at 95 °C for 10 min. The remainder of the supernatant was incubated with anti-FLAG M2 beads (Sigma, A2220) for 4 h at 4 °C. The beads were washed with coimmunoprecipitation buffer three times, and then the protein complexes were eluted with 2% SDS.

#### Western blot

Cell lysates or immunoprecipitated proteins were separated by SDS-PAGE and then transferred to nitrocellulose filter membranes. After blocking with 5% nonfat milk in TBST (10 mM Tris, 70 mM NaCl, pH 7.6, 0.1% Tween-20), the membranes were incubated with primary antibodies overnight at 4 °C, washed with TBST three times for 15 min each, and then incubated with the corresponding HRP-conjugated secondary antibodies for one hour at room temperature. Quantification of blots was performed using ImageJ software (NIH, Bethesda, MA).

#### Neuronal culture and transfection

Primary mouse cortical neuron cultures were prepared from E17.5 C57/B6L embryos as previously described [40]. Cortical tissues were dissected from embryos in precooled Hanks' Balanced Salt Solution (HBSS) and digested in prewarmed HBSS containing 0.025% trypsin (Gibco, 15090-046) at 37 °C for 20 min. Neurons were plated on poly-*D*-lysine (Sigma, P1024)-coated coverslips (200,000 cells/ml for 12-well plates, 500,000 cells/ml for 6-well plates). The cultures were maintained at 37 °C in 5% CO<sub>2</sub> in neurobasal medium (Gibco, 21103049) containing 1 × B27 (Gibco, 17504044), 1 × GlutaMAX (Thermo Fisher, 35050061), and 100 U/ml penicillin–streptomycin solution (Thermo Fisher, 15140148). After seven days in vitro (DIV), the cultured neurons were transfected with plasmids using Lipofectamine 2000 Transfection Reagent (Thermo Fisher, 11668019).

#### Immunofluorescence and image analysis

At four days after transfection, the cultured neurons were fixed with 4% paraformaldehyde (Polysciences, Warrington, PA; 04018-1) and 4% sucrose in PBS for 15 min at room temperature, followed by three washes with PBS. The cells were then incubated with primary antibody overnight at 4 °C, washed three times in PBS, and then incubated with secondary antibodies for 1 h at room temperature. Subsequently, the cells were washed three times in PBS and mounted in VECTASHIELD Mounting Media (Vector Labs, Newark, CA; H-1000). Z-stack images were acquired with a Zeiss LSM880 confocal microscope. Quantification of colocalized RAB3A/KIF1A

or VAMP2/KIF1A was performed with Imaris software (Oxford Instruments, Abingdon, United Kingdom).

### Statistical analysis

Statistical analysis was performed with SPSS 25.0. Descriptive statistics (mean  $\pm$  SD) were calculated for continuous variables. One-way ANOVA and Dunn's test were used to compare continuous variable data. For comparison of categorical variables, Fisher's exact test was applied. Association analysis of the RDVs was performed across the entire *KIF1A* gene and certain regions using Fisher's exact test, which was performed on an allelic basis. A *P* level of 0.05 was defined as the threshold of statistical significance.

## Results

### Mutation analysis of *KIF1A* in the ALS cohorts

To identify the possible association of *KIF1A* with ALS, we analyzed the WES data from 941 patients with ALS. Demographic and clinical characteristics are shown in Table 1. In this cohort, eight different candidate heterozygous RDVs in the *KIF1A* gene were identified in 10 unrelated patients, accounting for 1.06% of all patients (10/941). Among the 10 patients, two patients had family history of ALS, and the remaining patients were sporadic. The detailed information is listed in Additional file 1: Tables S2 and S3. Some RDVs deserve noticeable. The variant c.4760C>T; p.P1587L was identified in three unrelated sporadic patients (A737, A893, and A342). Notably, the c.4928C>T; p.A1643V variant was not found in any public database. We were unable to determine whether these variants were de novo variants, as samples from these patients' parents could not be obtained because the parents had died or were otherwise unavailable. In addition, the patient P1 (A148) who had the c.1108C>T; p.R370C variant also carried a stop-gain variant in the *CHCHD10* gene (NM\_213720:c.C312G; p.Y104X).

In the Project Mine, 18 different rare nonsynonymous variants in *KIF1A* were identified in 19 ALS patients, including 17 missense variants and one frameshift variant. In the ALSdb cohort, additional 15 different rare nonsynonymous variants in *KIF1A* were identified in 16

ALS patients, including 14 missense variants and one stop-gain variant. In total, 45 patients with different RDVs in the *KIF1A* coding sequence were found among 8624 patients with ALS. All missense variants were predicted to be deleterious by at least six of 11 in silico tools and had an MAF < 0.1% in the public databases. The details of these variants and pathogenicity predictions are listed in Additional file 1: Tables S2 and S3.

### Burden analysis at the *KIF1A* gene level and C-terminal region level

A total of 10 putative pathogenic variants were identified in 941 patients with ALS. Among the WES data for the 6708 East Asian control individuals in the gnomAD database v2, we identified 33 RDVs in *KIF1A* that fulfilled the same screening criteria (Additional file 1: Tables S2 and S3, Fig. S1). At the level of the entire *KIF1A* gene, gene burden testing was significant for *KIF1A* variants as a risk factor for ALS (Fisher's exact test, *P* = 0.036, odd ratio [OR] = 2.17, 95% confidence interval [CI] = 1.07 to 4.40). The *KIF1A* protein is composed of an N-terminal motor domain, four coiled coil (CC1-CC4) domains, with a Forkhead associated domain (FHA) following the second CC domain, and a C-terminal pleckstrin homology domain (PH) (<https://www.uniprot.org/>). Interestingly, we found that the variants in *KIF1A* associated with the ALS phenotype were mainly located in the C-terminal cargo-binding region. We therefore selected variants located in the C-terminal cargo-binding region (exons 24–47, amino acids 747–1690, with reference to transcript NM\_004321) for further statistical analysis. Finally, in the C-terminal region, we discovered nine variants in ALS patients and 18 variants in the East Asian control individuals without neurological disease in the gnomAD database v2. There was a significant association between variants in C-terminal regions and the ALS phenotype (Fisher's exact test, *P* = 0.004, OR = 3.58, 95%CI = 1.60–7.98). In the project Mine ALS cohort, burden analysis at the entire gene level and the C-terminal region level did not reach significant level (Table 2).

### Variants in *KIF1A* associated with ALS are distinct from variants associated with SPG30/HSAN2/MRD9

Mutations in *KIF1A* have been identified to cause SPG30, HSAN2, and MRD9. Considering the shared clinical manifestations between these diseases and ALS, the ALS patients with variants in *KIF1A* were carefully examined to rule out a misdiagnosis. Furthermore, the variants identified in our ALS cohort have not been reported in SPG30, HSAN2, or MRD9, except for the variant p.R370C, which has been reported in a patient with complex SPG [42]. The phenomenon of different phenotypes

**Table 1** Summary of demographic and clinical characteristics of ALS patients

	ALS cohort
No of ALS patients	941
Family history (+, %)	55, 5.84%
Sex (male, %)	616, 65.5%
Age at onset (years)	54.18 $\pm$ 10.83

**Table 2** Results of burden analysis at the *KIF1A* gene level in different cohorts

Cohort	Entire gene				C-terminal cargo-binding region			
	AC (patients)	AC (controls)	P value	OR [95% CI]	AC (patients)	AC (controls)	P value	OR [95% CI]
This study	10 (941)	33 (6708)	0.036*	2.17 [1.07–4.40]	9 (941)	18 (6708)	0.004*	3.58 [1.60–7.98]
Project Mine	19 (4366)	2 (1832)	0.053	4.00 [0.93–17.15]	17 (4366)	2 (1832)	0.079	3.57 [0.83–15.47]

AC, Allele count; CI, confidence interval; OR, odd ratio. \*P < 0.05

caused by the same variant in the *KIF1A* gene has also been described previously [27].

To further elucidate the relationship between *KIF1A* genotype and phenotype, we evaluated the locations of the ALS-related RDVs discovered in our study and pathogenetic variants related with other phenotypes (SPG30, HSN2, and MRD9) that have been reported in ClinVar (<https://www.ncbi.nlm.nih.gov/clinvar/>) (Fig. 1). Intriguingly, the variants associated with SPG and HSN were mostly located in the N-terminal motor domain of *KIF1A*, while the variants identified with the ALS phenotype in our study were located predominantly in the C-terminal cargo-binding region.

**Clinical characteristics of ALS patients with RDVs in *KIF1A***

The clinical manifestations of the 10 ALS patients carrying RDVs in *KIF1A* varied greatly. The mean AAO of the 10 patients was 56.70 ± 7.82 years, ranging from 40 to 67 years. The clinical features of patients with variants in different functional regions of *KIF1A* are summarized in Table 3 and Additional file 1: Table S4.

Interestingly, we found that these patients tended to display sensory disturbance (60.0%, 6/10).

Among these patients, two had a family history of ALS (Fig. 2). In Family 1, proband P4 (A707, III-4) harbored the variant c.3314G>A;p.R1105Q and showed early disease onset and long disease duration. His elder brother (III:2) carried the same variant and showed similar clinical features. The elder sister (III:1) did not harbor this variant and did not show neurological phenotypes at her last examination, at the age of 64. In Family 2, Patient P9 (A860) (III:2) harboring the variant p.A1643V showed a short survival time with an AAO of 50 years. His uncle (II:5) showed similar symptoms and died at age 38. The patient’s father did not show neurological symptoms or signs at the latest examination. Unfortunately, because DNA samples from the proband’s father and uncle were unavailable, we did not perform co-segregation analysis on this family.

The other eight patients all had sporadic ALS. Patients P6 (A737), P7 (A342) and P8 (A893) carried the same variant (p.P1587L) in *KIF1A* but showed

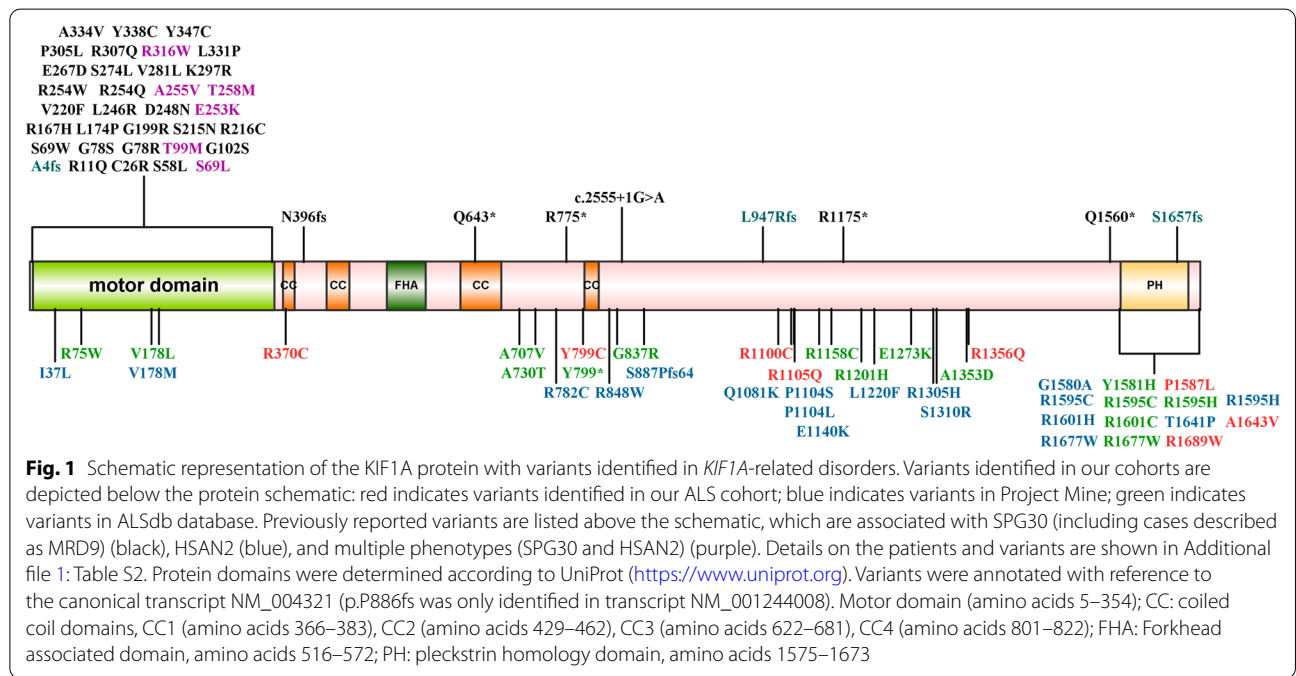
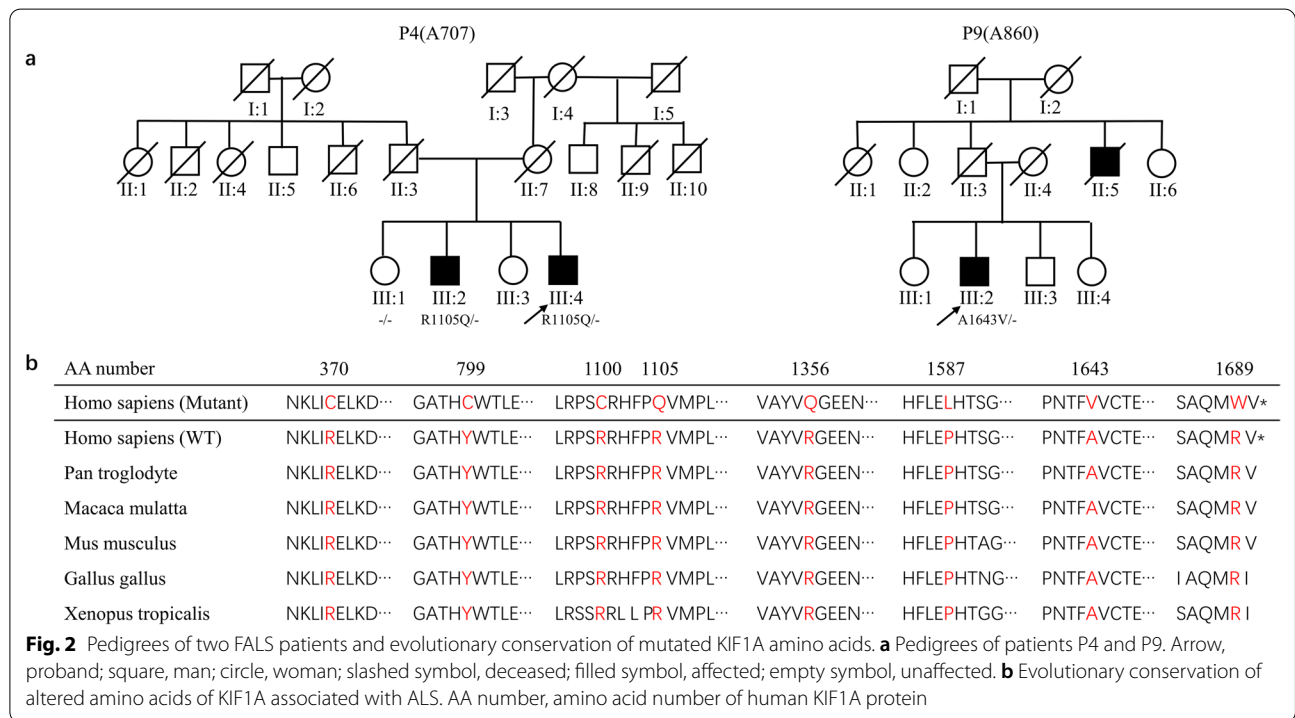


**Table 3** Clinical features of ALS patients with RDVs in the *KIF1A* gene

Patient ID	Sample ID	Amino acid change	Sex	Family history	Age at onset (years)	Survival time (months)	Alive (Y/N)	Site of onset	Cognition impairment	Sensory
RDV location (from CC1 to CC2)										
P1	A148	R370C	M	S	59	NA	NA	Spinal	NA	–
RDV location (between CC3 and PH)										
P2	A981	Y799C	M	S	56	50	N	Spinal	+	–
P3	A125	R1100C	F	S	66	28	N	Spinal	NA	+
P4	A707	R1105Q	M	AD	40	>84	Y	Spinal	–	+
P5	A054	R1356Q	F	S	63	>42	Y	Spinal	–	+
RDV location (PH domain)										
P6	A737	P1587L	M	S	59	>56	Y	Spinal	+	+
P7	A342	P1587L	M	S	50	>41	Y	Spinal	–	+
P8	A893	P1587L	M	S	67	29	N	Bulbar	–	+
P9	A860	A1643V	M	AD	50	32	N	Spinal	–	–
P10	A331	R1689W	M	S	57	>9	Y	Spinal	–	–

AD, autosomal dominant; F, female; M, male; N, no; NA, not available; S, sporadic; Y, yes; +, affected; –, not affected



different disease manifestations. The patient P6 (A737) was diagnosed with probable ALS 34 months after onset at the age of 59, and his motor symptoms were accompanied by cognitive impairment and sensory disturbance. The patient P7 (A342) showed similar manifestations. He was diagnosed with probable ALS 41 months after onset at the age of 53, and he also

showed sensory disturbance. The patient P8 (A893) showed a more severe phenotype, with a survival time of only 29 months; he also showed sensory disturbance but without cognitive impairment.

**ALS-associated missense variants of *KIF1A* enhance binding to cargos**

Next, we investigated the functional effects of several ALS-associated variants, among which Y799C, R1100C, R1356Q, P1587L, and A1643V are located in the C-terminal half of the protein, spanning from the CC3 to the PH domain, while R370C is located in CC1. To test whether these variants affect the protein level of

*KIF1A*, we generated constructs expressing wild-type (WT) or mutated form of human *KIF1A* and transfected these constructs into HEK293T cells. Immunoblotting showed comparable levels of the mutated *KIF1A* proteins to that of WT *KIF1A* (Fig. 3a, b), suggesting that these ALS-associated *KIF1A* variants do not alter protein abundance.

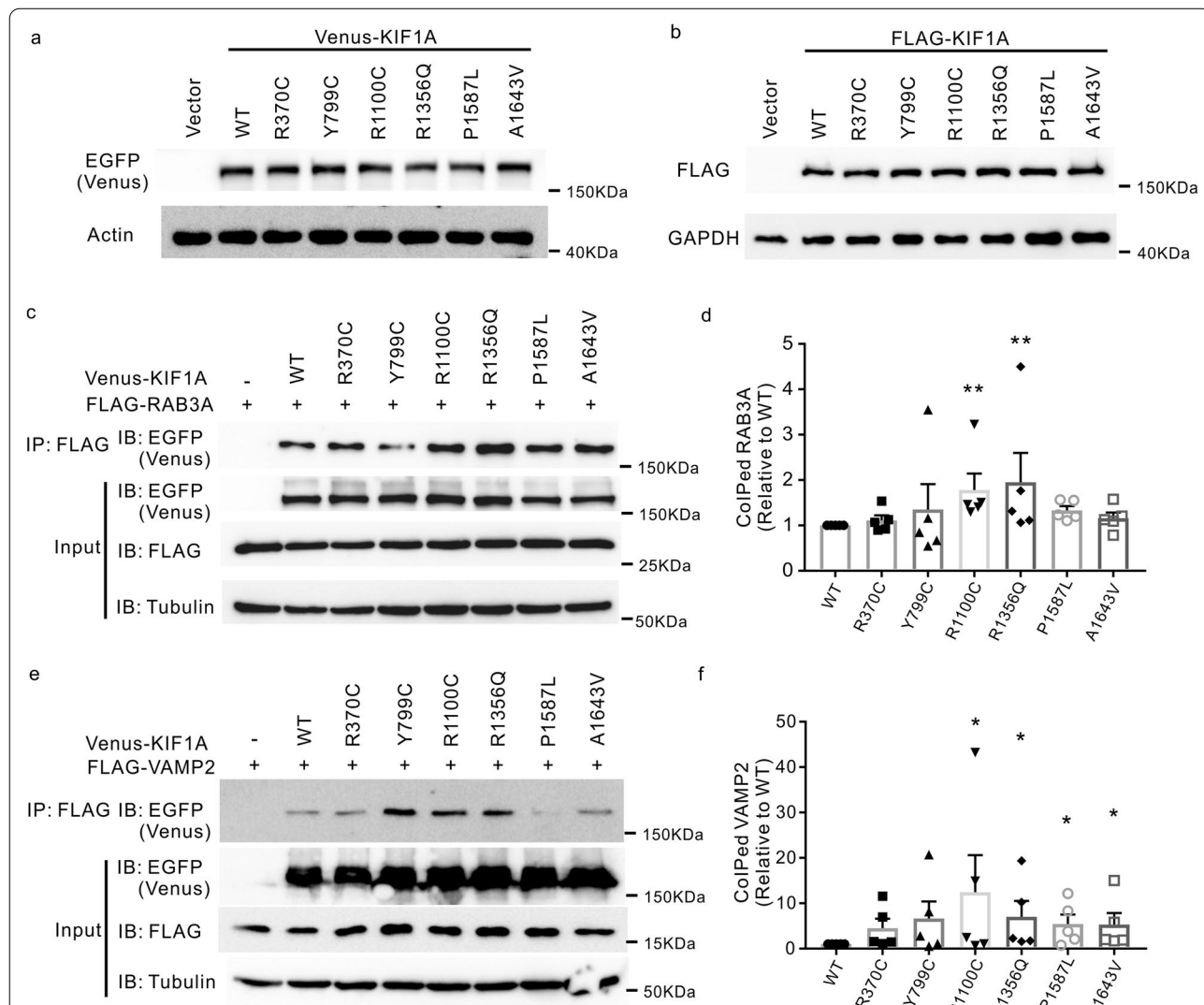


**Fig. 3** Binding of cargos to ALS-associated *KIF1A* mutants. **a, b** Plasmids expressing Venus- or FLAG-tagged WT and missense-mutation *KIF1A* were transfected into HEK293T cells. Cells were lysed and immunoblotted with antibodies against EGFP (to recognize Venus) or FLAG. **c, e** HEK293T cells were cotransfected with plasmids encoding FLAG-RAB3A or FLAG-VAMP2, along with plasmids encoding Venus-*KIF1A* WT, designated mutants, or empty vector. FLAG-RAB3A or FLAG-VAMP2 was immunoprecipitated with a FLAG antibody, and the immunoprecipitated proteins were identified by blotting with the indicated antibodies. **d** Quantification of immunoprecipitates in **c**. The intensity of coimmunoprecipitated RAB3A was normalized to the intensity of RAB3A input, and then the value for each mutant was normalized to WT.  $n = 5$  experiments.  $**P < 0.01$ .  $P = 0.0054$  (WT vs R1100C);  $P = 0.0084$  (WT vs R1356Q);  $P = 0.0570$  (WT vs P1587L);  $P = 0.3055$  (WT vs A1643V) by one-way ANOVA and Dunn's test. Error bars represent SEM. **f** Quantification of immunoprecipitates in **e**. Quantification was performed as described in **d**.  $n = 5$  experiments.  $*P < 0.05$ .  $P = 0.0281$  (WT vs R1100C);  $P = 0.0192$  (WT vs R1356Q);  $P = 0.0281$  (WT vs P1587L);  $P = 0.0281$  (WT vs A1643V) by one-way ANOVA and Dunn's test. Error bars represent SEM

Given that the ALS-related *KIF1A* variants were located predominantly at the C-terminal region, which preferably binds cargos, we sought to test whether these variants alter the binding affinity to cargo proteins. *KIF1A* is the primary kinesin motor that transports SVPs carrying synaptic vesicle proteins such as RAB3A, synaptophysin, and VAMP2 [20–22]. We expressed WT and mutant *KIF1A* tagged with Venus (a YFP variant) at the C-terminal together with FLAG-tagged RAB3A or FLAG-tagged VAMP2 in HEK293T cells and evaluated their coimmunoprecipitation with RAB3A or VAMP2. Strikingly, some *KIF1A* missense variants (including R1100C and R1356Q) showed increased binding to RAB3A (Fig. 3c, d, Additional file 1: Fig. S2). In addition, four *KIF1A* mutants (R1100C, R1356Q, P1587, and A1643V) displayed higher binding affinity to VAMP2 than WT *KIF1A* (Fig. 3e, f, Additional file 1: Fig. S3). Moreover, we assessed the binding of missense variants of *KIF1A* to synaptophysin by using coimmunoprecipitation in HEK293T cells. The binding affinity of *KIF1A* variant Y799C to synaptophysin was enhanced compared to that of WT (Additional file 1: Fig. S4).

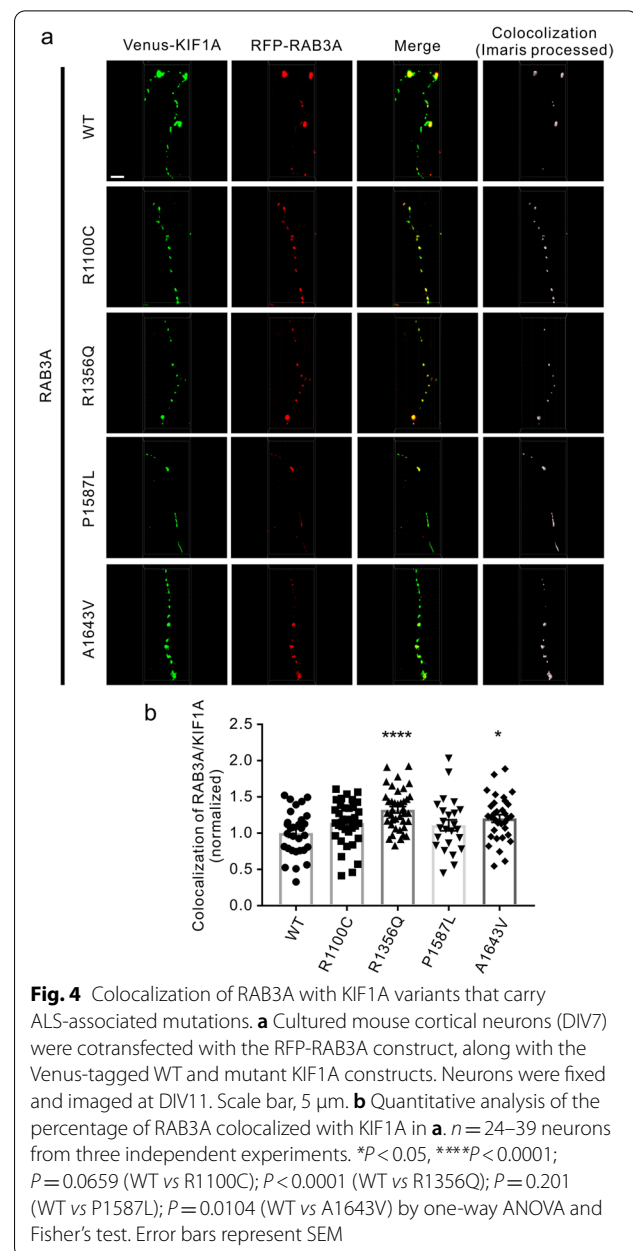
#### ALS-related *KIF1A* variants increase colocalization of *KIF1A* motor with SVPs in cultured neurons

We next asked whether the increased cargo-binding capacity of ALS-related *KIF1A* variants is associated with any change in the localization of presynaptic vesicles to the *KIF1A* motor. We cotransfected the RFP-RAB3A construct along with Venus-tagged mutant (R1100C, R1356Q, P1587L, and A1643V) or WT *KIF1A* into the cultured cortical neurons at DIV7 and analyzed the colocalization of SVPs (containing RAB3A) and *KIF1A* at DIV11. The results showed that the percentage of RAB3A colocalized with *KIF1A* was increased in neurons transfected with plasmids expressing the R1356Q and A1643V *KIF1A* mutants (Fig. 4a, b). The R1100C variant also increased the colocalization between RAB3A and *KIF1A*, although this increase did not reach statistical significance (Fig. 4a, b,  $P=0.0659$ ).

We performed a similar examination of the colocalization of SVPs carrying VAMP2 with the *KIF1A* motor. The R1356Q and A1643V variants increased the percentage of VAMP2 colocalized with *KIF1A* (Fig. 5a, b). Together, these data show that presynaptic vesicle precursors accumulate to ALS-associated mutated *KIF1A* motors.

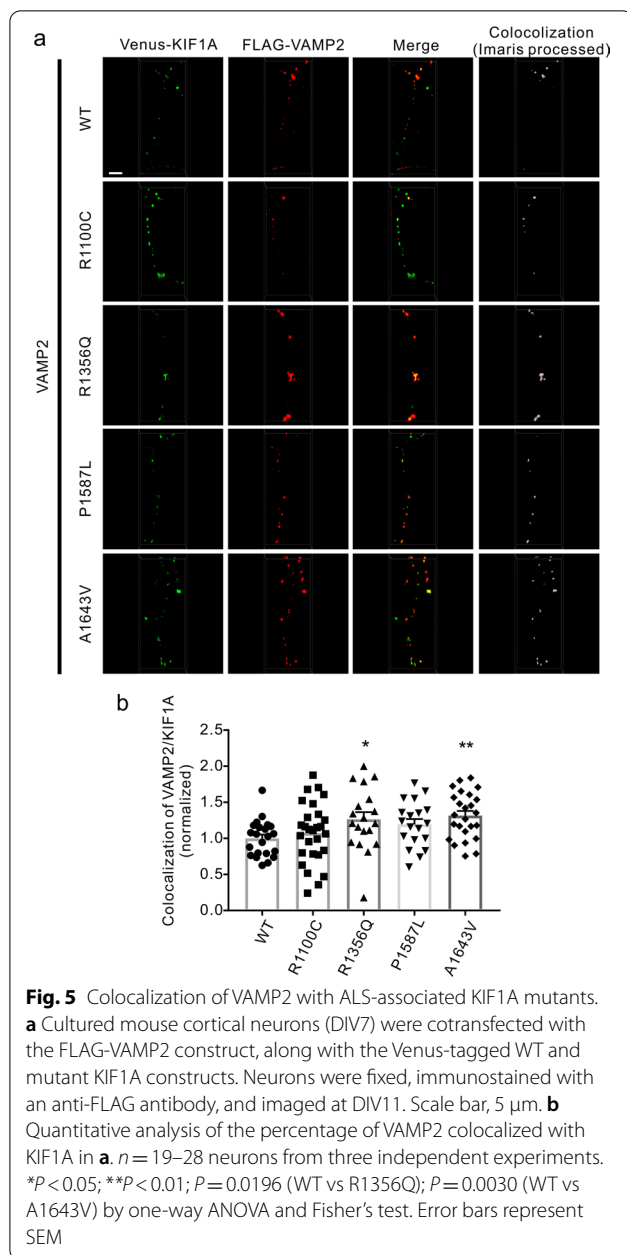
#### Discussion

Here, we provide clinical, genetic, and cell biological data to define a new *KIF1A*-associated phenotype of ALS. We identified eight variants in the *KIF1A* gene from 10 of 941 patients with ALS. The frequency of candidate RDVs in *KIF1A* suggested that *KIF1A* might be a common



causative or risk-conferring gene for ALS, especially when the variants are located in the C-terminal half of the protein, a cargo-binding region. However, the significant association of *KIF1A* gene with ALS was not replicated in the Project Mine ALS cohort. This may be caused by difference in genetic background, which is well recognized in ALS. For example, the expansion mutation in *C9orf72* is the most common genetic cause of ALS in Europe, but not in Asia. In addition, mutations in *KIF5A*, identified as a novel ALS gene in a European ancestry genome-wide analysis study, were rare in our ALS patients [2, 29].





In the present study, the ALS patients with RDVs in the *KIF1A* gene showed high clinical heterogeneity. The AAO ranged from 40 to 67 years, and the survival time ranged from more than 9 to more than 84 months. We noted several interesting genotype–phenotype correlation phenomena. For example, a same variant, R370C [42] or P1587L, is associated with different clinical manifestations. We speculate that the different phenotypes in these patients with P1587L might be caused by the difference in disease duration. That is, it is possible that patient P6 might show cognitive impairment with a longer survival

time. Interestingly, we found that ALS patients carrying RDVs in *KIF1A* tended to show sensory disturbance. Consistent with this observation, mutations in *KIF1A* have also been reported to cause HSAN, which affects sensory neurons. Etiologically, this could be explained by the various biological functions of the KIF1A protein. KIF1A is required for transportation of the neurotrophin receptor TrkA [24]. TrkA protein is implicated in the sensory pathway [43], and disruption of KIF1A-mediated axon transport of TrkA leads to sensory neuron loss [23]. Therefore, we speculate that the ALS-related variants in *KIF1A* might have diverse functional impacts that result in sensory disturbance in ALS patients.

Notably, we also identified one patient who carried RDV in other ALS pathogenic genes. In addition to p.R370C in *KIF1A*, patient P1 (A148) also carried a c.C312G; p.Y104X variant in the *CHCHD10* gene. This patient showed upper limb and neck weakness and atrophy six months after onset. More detailed clinical information was not available due to the loss of follow-up. The frequency of the c.C312G; p.Y104X variant in the public databases was less than 0.01% and functional prediction suggested pathogenic or uncertain significance in ClinVar. In this patient, the RDV in *KIF1A* and RDVs in other causative genes may both contribute to the pathogenesis of ALS. These results are in line with the oligogenic genetic model of ALS.

Our present results, along with other findings, suggest that *KIF1A* might be a shared causative gene for SPG, HSAN, and ALS. Some other common causative genes for these different types of disease have been reported. For example, pathogenic mutations in either *KIF5A* or *SPG11* lead to SPG and ALS [28–31], and mutations in the *SPTLC1* gene lead to HSAN and ALS [32, 33, 44]. Interestingly, the *KIF1A*-associated HSAN and MRD phenotypes have also been recognized to be mild phenotypes of complex SPG [27]. Therefore, we hypothesize that HSAN, SPG, and ALS may represent a continuum of phenotypes associated with variants in the *KIF1A* gene. As is the case for *NOTCH2NLC*, *C9ORF72*, and *PRRT2* genes, the clinical spectrum of *KIF1A*-related disease varies greatly [37, 45, 46], giving rise to a large number of “*KIF1A*-related disorders”. The high clinical heterogeneity of “*KIF1A*-related disorders” may be explained by multiple etiological mechanisms, such as the multiple biological functions of the KIF1A protein, potential modifying genes, and epigenetic and environmental factors.

Consistent with previous studies of *KIF5A* [29, 47], we found that most variants within the KIF1A C-terminal cargo-binding domain are related to ALS, while the majority of missense variants at the N-terminal motor domain are related to SPG. The variety of clinical phenotypes may be caused by the different changes in function

caused by variants in different regions of KIF1A. Our results highlight the importance of the cargo-binding activity of the kinesin motor in ALS pathogenesis. Precise regulation of motor-cargo interactions is critical for cargo recruitment, transport efficiency and specificity, and thus for modulating the temporal and spatial distribution of the cargos. Thus far, it is still unclear how cargo recognition, binding, transport, and detachment affect ALS symptoms. In this study, the biochemical and cellular biological examinations revealed that the ALS-related *KIF1A* variants modulate motor-cargo interactions and alter the colocalization of SVPs with the KIF1A motor in neurons. These findings suggest that the disease-associated variants indeed regulate the physiological role of kinesin motors. As KIF1A transports many types of cargo, including SVPs, DCVs, and lysosomes, alterations in the interaction with any cargo might contribute to ALS symptoms. Thus, further comprehensive investigations into the binding and transportation of a wide range of cargos are needed to dissect the pathogenic mechanisms of ALS-associated variants.

In this study, our results revealed that the ALS-related *KIF1A* variants might promote binding to cargos, implicating a gain of function for *KIF1A* variants. Previous results have identified relationships between diseases and gain-of-function mutations in genes involved in axonal transport, such as *SPG30* and *KIF1A*, congenital fibrosis of the extraocular muscle type 1 and *KIF21A*, and autosomal dominant lower extremity-predominant spinal muscular atrophy-2A and *BICD2* [48–51]. In addition, a missense mutation in the *Dync1h1* (cytoplasmic dynein heavy chain 1) gene causes progressive motor neuron degeneration in mice [52] and enhances binding to the dynein light intermediate and intermediate chains [53]. We show here that the ALS-related *KIF1A* variants located at the C-terminal increase SVP binding and recruit more SVPs, suggesting that these variants are gain-of-function rather than loss-of-function mutations. Together, these studies indicate that the balance of tightly regulated axon transport events is essential for neuron physiology and survival. It is likely that the abnormal accumulation of SVPs or other KIF1A cargos caused by ALS-related *KIF1A* missense variants is deleterious and neurotoxic, eventually resulting in neurodegeneration.

Autoinhibition is a common mechanism for regulation of Kinesin motor activity, such as KIF1A and KIF5A. Recently, ALS-related mutations in KIF5A have been reported to result in a lack of autoinhibition, leading to a toxic gain of function [54]. KIF5A is autoinhibited by a direct intramolecular interaction between its C-terminal isoleucine-alanine-lysine (IAK) motif and the N-terminal motor domain. ALS-related mutation within the KIF5A C-terminal region disrupts the autoinhibition

and leads to a constitutively activated motor. In contrast, current studies have suggested that the CC2-FHA-CC3 region serve as a regulatory region of KIF1A to modulate autoinhibition and dimerization of molecular motor [55–57]. As most of the ALS-associated *KIF1A* variants identified in this study locate at the C-terminal CC4-PH region that is supposed to bind cargo, we did not test the effect of these mutations on autoinhibition. However, it is possible that further genetic studies may identify more ALS-related mutations that regulate motor autoinhibition. The putative mechanism involving autoinhibition and its relation to ALS pathogenesis needs more investigations.

In this study, we tested the cargo-binding capacity of six ALS-related *KIF1A* point mutations. Results indicated a variability in the effect of these mutations on cargo binding, likely because that these mutations locate at different domains of KIF1A motor. Several studies have dissected the role of different KIF1A domains in cargo binding. For example, Hummel et al. showed that CC4 and PH regions are required for KIF1A-cargo interaction [57]; Stucchi et al. reported that the stalk domain of KIF1A (amino acids 657–1105) interacts with Liprin-a and TANC2 to help DCV trafficking [24]. However, the exact binding regions for different cargos remain largely unclear. We found that R1100C and R1356Q, which locate between regions CC4 and PH, alter the interaction with RAB3A and VAMP2. In addition, P1587L and A1643V that locate at the PH domain also alter the binding to VAMP2, while moderately affecting binding to RAB3A ( $P=0.0570$ , P1587L;  $P=0.3055$ , A1643V). These findings support the notion that CC4 and PH, as well as the region between them, interact with cargos. Moreover, we also noted that several variants, such as R370C, are located in the CC1 region. It has been reported that the CC1 domain does not bind to cargos but regulates dimerization [58, 59]. Consistently, we found that the R370C variant did not exhibit altered binding to SVP cargo proteins in co-immunoprecipitation experiments. The R370C variant might contribute to ALS pathogenesis through a mechanism distinct from that of other variants.

Our study had certain limitations. First, principal component analysis was not performed on the entire cohort to demonstrate the similar ethnic background between patients and controls. Second, the size of the cohort was relatively small compared to other studies of genome-wide variants in ALS. In addition, the  $P$ -values identified in this study would not reach statistical significance if in a genome-wide study. However, burden analysis in genome-wide studies did not always identify all known ALS causative or risk genes as ALS-associated genes. In a word, it requires more studies to validate the association of *KIF1A* with ALS. Third, due to the late onset of

ALS, many family members of the patients in our study were unavailable for co-segregation analysis. Therefore, we were not able to determine whether these variants were de novo variants. Fourth, the sensory disturbance was evaluated only based on subjective description, and quantitative sensory tests were not performed; thus, this relationship of variants in *KIF1A* and sensory disturbance should be verified in the future. Last, in the present study, we conducted only a preliminary functional assay of cargo binding in cultured cells. Careful examination of whether these ALS-related *KIF1A* variants lead to neurodegenerative conditions and neuron loss in animal models will help to further clarify the pathogenic consequences and their relevance to ALS.

## Conclusions

In summary, our study highlights the importance of *KIF1A* motor-mediated transport in the pathogenesis of ALS, indicating *KIF1A* as an important player in the oligogenic scenario of ALS.

## Abbreviations

AAO: Age at onset; ALS: Amyotrophic lateral sclerosis; CC: Coiled coil; DCV: Dense core vesicle; FALS: Familial ALS; FHA: Forkhead associated domain; HSAN: Hereditary sensory and autonomic neuropathy type; MAF: Minor allele frequency; MRD: Mental retardation type; PH: Pleckstrin homology domain; RDVs: Rare damage variants; SALS: Sporadic ALS; SPG: Spastic paraplegia; SVPs: Presynaptic vesicle precursors; WES: Whole-exome sequencing.

## Supplementary Information

The online version contains supplementary material available at <https://doi.org/10.1186/s40035-022-00320-2>.

**Additional file 1: Fig. S1.** Schematic representation of the *KIF1A* protein with the RDVs identified in controls. **Fig. S2.** Interaction between RAB3A and the *KIF1A* motor. **Fig. S3.** Interaction between VAMP2 and the *KIF1A* motor. **Fig. S4.** ALS-associated *KIF1A* variants alter binding to synaptophysin. **Table S1.** Primers in constructing plasmid. **Table S2.** Details of RDVs in the *KIF1A* gene identified in ALS patients and healthy controls. **Table S3.** In-silico pathogenicity predictions for RDVs in the *KIF1A* gene. **Table S4.** Clinical features in ALS patients carrying RDVs in the *KIF1A* gene.

## Acknowledgements

We are grateful to the patients for their participation in this study.

## Author contributions

PL and YY performed the majority of the analyses and wrote the manuscript. ZL contributed to the bioinformatic analyses. XH and WL contributed to the collection of detailed clinical data. JW and KZ contributed to functional examination. BJ, LS, HJ, and JG contributed to the clinical part of the project. BT and ZZ supervised the analyses. ZH and JW coordinated the study and wrote the manuscript. All authors read and approved the final manuscript.

## Funding

This work was supported by the National Key R&D Program of China (2021YFA0805200), the National Major Projects in Brain Science and Brain-like Research (2021ZD0201803 to J.W.), the National Natural Science Foundation of China (82171431, 81671120, 81300981 to J.W., 31872778 and 82171506 to Z.H.), the National Key Research and Development Program of China (#2018YFC1312003 to J.W.), the Natural Science Fund for Distinguished Young

Scholars of Hunan Province, China (2020JJ2057 to J.W.), the Project Program of National Clinical Research Center for Geriatric Disorders at Xiangya Hospital (2020LNJJ13 to J.W.), Key Research and Development Programs from Hunan Province (2021DK2001 to Z.H.), the Innovative Team Program from Hunan Province (2019RS1010), the Innovation-driven Team Project from Central South University (2020CX016), and the Discipline Innovative Engineering Plan (111 Program) of China (B13036). Z.H. is supported by the Hunan Hundred Talents Program for Young Outstanding Scientists.

## Availability of data and materials

Data analyzed in this study are available from the corresponding authors upon reasonable request. In addition, the genetic variation data have been submitted to dbSNP.

## Declarations

### Ethics approval and consent to participate

This study was approved by the Ethics Committee of Xiangya Hospital of Central South University in China (approval No. 202103191). Written informed consent was obtained from all individuals.

### Consent for publication

Written informed consent for publication was obtained from individuals described with personal details.

### Competing interests

The authors declare no competing financial interests.

## Author details

<sup>1</sup>Hunan Key Laboratory of Molecular Precision Medicine, Department of Critical Care Medicine, Xiangya Hospital, Central South University, Changsha 410008, China. <sup>2</sup>Department of Neurology, Xiangya Hospital, Central South University, Changsha 410008, China. <sup>3</sup>National Clinical Research Center for Geriatric Diseases, Xiangya Hospital, Central South University, Changsha 410008, China. <sup>4</sup>Key Laboratory of Hunan Province in Neurodegenerative Disorders, Central South University, Changsha 410008, China. <sup>5</sup>Center for Medical Genetics, School of Life Sciences, Central South University, Changsha 410008, China. <sup>6</sup>Engineering Research Center of Hunan Province in Cognitive Impairment Disorders, Central South University, Changsha 410008, China. <sup>7</sup>Hunan International Scientific and Technological Cooperation Base of Neurodegenerative and Neurogenetic Diseases, Changsha 410008, China. <sup>8</sup>Hunan Provincial Clinical Research Center for Critical Care Medicine, Xiangya Hospital, Central South University, Changsha 410008, China. <sup>9</sup>Hunan Key Laboratory of Animal Models for Human Diseases, School of Life Sciences, Central South University, Changsha 410008, China.

Received: 27 April 2022 Accepted: 10 October 2022

Published online: 26 October 2022

## References

- van Es MA, Hardiman O, Chio A, Al-Chalabi A, Pasterkamp RJ, Veldink JH, et al. Amyotrophic lateral sclerosis. *Lancet*. 2017;390(10107):2084–98.
- Liu Z, Yuan Y, Wang M, Ni J, Li W, Huang L, et al. Mutation spectrum of amyotrophic lateral sclerosis in Central South China. *Neurobiol Aging*. 2021;107:181–8.
- Chia R, Chiò A, Traynor BJ. Novel genes associated with amyotrophic lateral sclerosis: diagnostic and clinical implications. *Lancet Neurol*. 2018;17(1):94–102.
- Oskarsson B, Horton DK, Mitsumoto H. Potential environmental factors in amyotrophic lateral sclerosis. *Neurol Clin*. 2015;33(4):877–88.
- Talbott EO, Malek AM, Lacomis D. The epidemiology of amyotrophic lateral sclerosis. *Handb Clin Neurol*. 2016;138:225–38.
- Taylor JP, Brown RH Jr, Cleveland DW. Decoding ALS: from genes to mechanism. *Nature*. 2016;539(7628):197–206.
- Castellanos-Montiel MJ, Chaineau M, Durcan TM. The neglected genes of ALS: cytoskeletal dynamics impact synaptic degeneration in ALS. *Front Cell Neurosci*. 2020;14: 594975.

8. Suzuki N, Akiyama T, Warita H, Aoki M. Omics approach to axonal dysfunction of motor neurons in amyotrophic lateral sclerosis (ALS). *Front Neurosci.* 2020;14:194.
9. Guo W, Vandoorne T, Steyaert J, Staats KA, Van Den Bosch L. The multifaceted role of kinases in amyotrophic lateral sclerosis: genetic, pathological and therapeutic implications. *Brain.* 2020;143(6):1651–73.
10. Bilsland LG, Sahai E, Kelly G, Golding M, Greensmith L, Schiavo G. Deficits in axonal transport precede ALS symptoms in vivo. *Proc Natl Acad Sci U S A.* 2010;107(47):20523–8.
11. Tian F, Yang W, Mordes DA, Wang JY, Salameh JS, Mok J, et al. Monitoring peripheral nerve degeneration in ALS by label-free stimulated Raman scattering imaging. *Nat Commun.* 2016;7:13283.
12. Warita H, Itoyama Y, Abe K. Selective impairment of fast anterograde axonal transport in the peripheral nerves of asymptomatic transgenic mice with a G93A mutant SOD1 gene. *Brain Res.* 1999;819(1–2):120–31.
13. Kieran D, Hafezparast M, Bohnert S, Dick JR, Martin J, Schiavo G, et al. A mutation in dynein rescues axonal transport defects and extends the life span of ALS mice. *J Cell Biol.* 2005;169(4):561–7.
14. Sasaki S, Iwata M. Impairment of fast axonal transport in the proximal axons of anterior horn neurons in amyotrophic lateral sclerosis. *Neurology.* 1996;47(2):535–40.
15. Osking Z, Ayers JL, Hildebrandt R, Skruker K, Brown H, Ryu D, et al. ALS-linked SOD1 mutants enhance neurite outgrowth and branching in adult motor neurons. *iScience.* 2019;11:294–304.
16. Fischer LR, Culver DG, Tennant P, Davis AA, Wang M, Castellano-Sanchez A, et al. Amyotrophic lateral sclerosis is a distal axonopathy: evidence in mice and man. *Exp Neurol.* 2004;185(2):232–40.
17. Encalada SE, Goldstein LS. Biophysical challenges to axonal transport: motor-cargo deficiencies and neurodegeneration. *Annu Rev Biophys.* 2014;43:141–69.
18. Maday S, Twelvetrees AE, Moughamian AJ, Holzbaur EL. Axonal transport: cargo-specific mechanisms of motility and regulation. *Neuron.* 2014;84(2):292–309.
19. Hirokawa N, Noda Y, Tanaka Y, Niwa S. Kinesin superfamily motor proteins and intracellular transport. *Rev Mol Cell Biol.* 2009;10(10):682–96.
20. Niwa S, Tanaka Y, Hirokawa N. KIF1Bbeta- and KIF1A-mediated axonal transport of presynaptic regulator Rab3 occurs in a GTP-dependent manner through DENN/MADD. *Nat Cell Biol.* 2008;10(11):1269–79.
21. Guedes-Dias P, Nirschl JJ, Abreu N, Tokito MK, Janke C, Magiera MM, et al. Kinesin-3 responds to local microtubule dynamics to target synaptic cargo delivery to the presynapse. *Curr Biol.* 2019;29(2):268–82.
22. Okada Y, Yamazaki H, Sekine-Aizawa Y, Hirokawa N. The neuron-specific kinesin superfamily protein KIF1A is a unique monomeric motor for anterograde axonal transport of synaptic vesicle precursors. *Cell.* 1995;81(5):769–80.
23. Tanaka Y, Niwa S, Dong M, Farkhondeh A, Wang L, Zhou R, et al. The molecular motor KIF1A transports the TrkA neurotrophin receptor and is essential for sensory neuron survival and function. *Neuron.* 2016;90(6):1215–29.
24. Stucchi R, Plucinska G, Hummel JJA, Zahavi EE, Guerra San JJ, Klykov O, et al. Regulation of KIF1A-driven dense core vesicle transport: Ca(2+)-/CaM controls DCV binding and liprin-alpha/TANC2 recruits DCVs to postsynaptic sites. *Cell Rep.* 2018;24(3):685–700.
25. Lo KY, Kuzmin A, Unger SM, Petersen JD, Silverman MA. KIF1A is the primary anterograde motor protein required for the axonal transport of dense-core vesicles in cultured hippocampal neurons. *Neurosci Lett.* 2011;491(3):168–73.
26. Yonekawa Y, Harada A, Okada Y, Funakoshi T, Kanai Y, Takei Y, et al. Defect in synaptic vesicle precursor transport and neuronal cell death in KIF1A motor protein-deficient mice. *J Cell Biol.* 1998;141(2):431–41.
27. Nicita F, Ginevrino M, Travaglini L, D'Arrigo S, Zorzi G, Borgatti R, et al. Heterozygous KIF1A variants underlie a wide spectrum of neurodevelopmental and neurodegenerative disorders. *J Med Genet.* 2021;58(7):475–83.
28. Stevanin G, Santorelli FM, Azzedine H, Coutinho P, Chomilier J, Denora PS, et al. Mutations in SPG11, encoding spatacsin, are a major cause of spastic paraplegia with thin corpus callosum. *Nat Genet.* 2007;39(3):366–72.
29. Nicolas A, Kenna KP, Renton AE, Ticozzi N, Faghri F, Chia R, et al. Genome-wide analyses identify KIF5A as a novel ALS gene. *Neuron.* 2018;97(6):1268–1283.e1266.
30. Reid E, Kloos M, Ashley-Koch A, Hughes L, Bevan S, Svenson IK, et al. A kinesin heavy chain (KIF5A) mutation in hereditary spastic paraplegia (SPG10). *Am J Hum Genet.* 2002;71(5):1189–94.
31. Orlicchio A, Babalini C, Borreca A, Patrono C, Massa R, Basaran S, et al. SPATACSIN mutations cause autosomal recessive juvenile amyotrophic lateral sclerosis. *Brain.* 2010;133(Pt 2):591–8.
32. Johnson JO, Chia R, Miller DE, Li R, Kumaran R, Abramzon Y, et al. Association of variants in the SPTLC1 gene with juvenile amyotrophic lateral sclerosis. *JAMA Neurol.* 2021;78:1236.
33. Mohassel P, Donkervoort S, Lone MA, Nalls M, Gable K, Gupta SD, et al. Childhood amyotrophic lateral sclerosis caused by excess sphingolipid synthesis. *Nat Med.* 2021;27(7):1197–204.
34. Wvea R. Project MinE: study design and pilot analyses of a large-scale whole-genome sequencing study in amyotrophic lateral sclerosis. *Eur J Hum Genet.* 2018;26(10):1537–46.
35. van der Spek RAA, van Rheenen W, Pulit SL, Kenna KP, van den Berg LH, Veldink JH. The project MinE databrowser: bringing large-scale whole-genome sequencing in ALS to researchers and the public. *Amyotroph Lateral Scler Frontotemporal Degener.* 2019;20(5–6):432–40.
36. Cirulli ET, Lasseigne BN, Petrovski S, Sapp PC, Dion PA, LeBlond CS, et al. Exome sequencing in amyotrophic lateral sclerosis identifies risk genes and pathways. *Science.* 2015;347(6229):1436–41.
37. Tian Y, Wang JL, Huang W, Zeng S, Jiao B, Liu Z, et al. Expansion of human-specific GGC repeat in neuronal intranuclear inclusion disease-related disorders. *Am J Hum Genet.* 2019;105(1):166–76.
38. Li J, Zhao T, Zhang Y, Zhang K, Shi L, Chen Y, et al. Performance evaluation of pathogenicity-computation methods for missense variants. *Nucleic Acids Res.* 2018;46(15):7793–804.
39. Hu Z, Yu D, Gu QH, Yang Y, Tu K, Zhu J, et al. miR-191 and miR-135 are required for long-lasting spine remodelling associated with synaptic long-term depression. *Nat Commun.* 2014;5:3263.
40. Ren M, Hu Z, Chen Q, Jaffe A, Li Y, Sadashivaiah V, et al. KCNH2-3.1 mediates aberrant complement activation and impaired hippocampal-medial prefrontal circuitry associated with working memory deficits. *Mol Psychiatry.* 2020;25(1):206–29.
41. Granseth B, Odermatt B, Royle SJ, Lagnado L. Clathrin-mediated endocytosis is the dominant mechanism of vesicle retrieval at hippocampal synapses. *Neuron.* 2006;51(6):773–86.
42. Vecchia SD, Tessa A, Dosi C, Baldacci J, Pasquariello R, Antenora A, et al. Monoallelic KIF1A-related disorders: a multicenter cross sectional study and systematic literature review. *J Neurol.* 2022;269(1):437–50.
43. Lei L, Laub F, Lush M, Romero M, Zhou J, Luikart B, et al. The zinc finger transcription factor Klf7 is required for TrkA gene expression and development of nociceptive sensory neurons. *Genes Dev.* 2005;19(11):1354–64.
44. Riviere JB, Ramalingam S, Lavastre V, Shekarabi M, Holbert S, Lafontaine J, et al. KIF1A, an axonal transporter of synaptic vesicles, is mutated in hereditary sensory and autonomic neuropathy type 2. *Am J Hum Genet.* 2011;89(2):219–30.
45. van der Ende EL, Jackson JL, White A, Seelaar H, van Blitterswijk M, Van Swieten JC. Unravelling the clinical spectrum and the role of repeat length in C9ORF72 repeat expansions. *J Neurol Neurosurg Psychiatry.* 2021;92(5):502–9.
46. Ebrahimi-Fakhari D, Saffari A, Westenberger A, Klein C. The evolving spectrum of PRRT2-associated paroxysmal diseases. *Brain.* 2015;138(Pt 12):3476–95.
47. Brenner D, Yilmaz R, Muller K, Grehl T, Petri S, Meyer T, et al. Hot-spot KIF5A mutations cause familial ALS. *Brain.* 2018;141(3):688–97.
48. Chiba K, Takahashi H, Chen M, Obinata H, Arai S, Hashimoto K, et al. Disease-associated mutations hyperactivate KIF1A motility and anterograde axonal transport of synaptic vesicle precursors. *Proc Natl Acad Sci U S A.* 2019;116(37):18429–34.
49. Huynh W, Vale RD. Disease-associated mutations in human BICD2 hyperactivate motility of dynein-dynactin. *J Cell Biol.* 2017;216(10):3051–60.
50. Cheng L, Desai J, Miranda CJ, Duncan JS, Qiu W, Nugent AA, et al. Human CFEOM1 mutations attenuate KIF21A autoinhibition and cause oculomotor axon stalling. *Neuron.* 2014;82(2):334–49.
51. van der Vaart B, van Riel WE, Doodhi H, Kevenaer JT, Katrukha EA, Gumy L, et al. CFEOM1-associated kinesin KIF21A is a cortical microtubule growth inhibitor. *Dev Cell.* 2013;27(2):145–60.

52. Hafezparast M, Klocke R, Ruhrberg C, Marquardt A, Ahmad-Annur A, Bowen S, et al. Mutations in dynein link motor neuron degeneration to defects in retrograde transport. *Science*. 2003;300(5620):808–12.
53. Deng W, Garrett C, Dombert B, Soura V, Banks G, Fisher EM, et al. Neurodegenerative mutation in cytoplasmic dynein alters its organization and dynein-dynactin and dynein-kinesin interactions. *J Biol Chem*. 2010;285(51):39922–34.
54. Baron DM, Fenton AR, Saez-Atienzar S, Giampetruzzi A, Sreeram A, Shankaracharya, et al. ALS-associated KIF5A mutations abolish autoinhibition resulting in a toxic gain of function. *Cell Rep*. 2022;39(1):110598.
55. Huo L, Yue Y, Ren J, Yu J, Liu J, Yu Y, et al. The CC1-FHA tandem as a central hub for controlling the dimerization and activation of kinesin-3 KIF1A. *Structure*. 2012;20(9):1550–61.
56. Niwa S, Lipton DM, Morikawa M, Zhao C, Hirokawa N, Lu H, et al. Autoinhibition of a neuronal kinesin UNC-104/KIF1A regulates the size and density of synapses. *Cell Rep*. 2016;16(8):2129–41.
57. Hummel JJA, Hoogenraad CC. Specific KIF1A-adaptor interactions control selective cargo recognition. *J Cell Biol*. 2021;220(10):e202105011.
58. Soppina V, Norris SR, Dizaji AS, Kortus M, Veatch S, Peckham M, et al. Dimerization of mammalian kinesin-3 motors results in superprocessive motion. *Proc Natl Acad Sci U S A*. 2014;111(15):5562–7.
59. Hammond JW, Cai D, Blasius TL, Li Z, Jiang Y, Jih GT, et al. Mammalian Kinesin-3 motors are dimeric in vivo and move by processive motility upon release of autoinhibition. *PLoS Biol*. 2009;7(3): e72.

Ready to submit your research? Choose BMC and benefit from:

- fast, convenient online submission
- thorough peer review by experienced researchers in your field
- rapid publication on acceptance
- support for research data, including large and complex data types
- gold Open Access which fosters wider collaboration and increased citations
- maximum visibility for your research: over 100M website views per year

At BMC, research is always in progress.

Learn more [biomedcentral.com/submissions](https://biomedcentral.com/submissions)

